

RESEARCH ARTICLE

# Pore size-mediated macrophage M1 to M2 transition affects osseointegration of 3D-printed PEEK scaffolds

Xiaopeng Yang<sup>1,2</sup>, Jianbo Gao<sup>2</sup>, Shenyu Yang<sup>2</sup>, Yan Wu<sup>2</sup>, Huilong Liu<sup>2</sup>, Danyang Su<sup>2</sup>, Dichen Li<sup>1\*</sup>

<sup>1</sup>State Key Lab for Manufacturing Systems Engineering, Xi'an Jiaotong University, Xi'an 710049, China

<sup>2</sup>The First Affiliated Hospital of Zhengzhou University, Zhengzhou 450052, China

## Abstract

Increasing evidence indicates that macrophages play an important role in angiogenesis and bone regeneration. Because the phenotypic polarization of macrophage is extremely sensitive to the pore size of materials, poly(ether-ether-ketone) (PEEK) scaffolds with pore sizes of 0, 200, and 400  $\mu\text{m}$  were prepared, and the influence of pore size-mediated macrophage polarization on subsequent angiogenesis and osteogenesis was examined. The interaction results of macrophages and scaffolds indicated that macrophages were responsive to the pore size of three-dimensional (3D)-printed PEEK scaffolds, and large pore size scaffolds showed greater potential in inducing M1 to M2 transition of macrophage and enhanced macrophage secretion of high concentrations of osteogenesis-related and angiogenesis-related cytokines. When human umbilical vein endothelial cells (HUVECs) and bone marrow mesenchymal stem cells (BMSCs) were cultured in the conditioned medium derived from co-culture of macrophages and scaffolds, HUVECs showed good angiogenic responses in terms of cell migration and angiogenic gene expression, while BMSCs showed good osteogenic differentiation effect in *in vitro* mineralization and osteogenesis-related gene expression. The results of bone defect repair showed that the bone volume/total volume ratio and trabecular thickness of the large pore size PEEK scaffold were significantly higher, and it had better biomechanical properties and achieved a better osseointegration effect. Our data demonstrate that large-pore PEEK scaffolds promote angiogenesis and osteogenic differentiation *in vitro* and osseointegration *in vivo*, most likely because scaffolds with larger pore size are able to mediate a higher degree of M1 to M2 transition in macrophages.

**\*Corresponding author:**

Dichen Li (dcli@mail.xjtu.edu.cn)

**Citation:** Yang X, Gao J, Yang S, *et al.*, 2023, Pore size-mediated macrophage M1 to M2 transition affects osseointegration of 3D-printed PEEK scaffolds. *Int J Bioprint*, 9(5): 755. <https://doi.org/10.18063/ijb.755>

**Received:** December 1, 2022

**Accepted:** February 12, 2023

**Published Online:** May 17, 2023

**Copyright:** © 2023 Author(s).

This is an Open Access article distributed under the terms of the Creative Commons Attribution License, permitting distribution, and reproduction in any medium, provided the original work is properly cited.

**Publisher's Note:** Whioce Publishing remains neutral with regard to jurisdictional claims in published maps and institutional affiliations.

**Keywords:** PEEK; 3D printing; Pore size, Macrophage, Osseointegration

## 1. Introduction

In the past decades, in order to improve the osseointegration ability of bone repair materials with host bone, researchers have mainly focused on designing or modifying bone repair materials to induce differentiation of bone marrow mesenchymal stem cells (BMSCs) into osteoblasts<sup>[1,2]</sup>. However, when the bone repair material is implanted

into the body as a foreign body, the immune system is first activated, and then a large number of cytokines and signaling protein molecules are released in response to the changes in the immune microenvironment around the bone repair material<sup>[3-5]</sup>. As an important part of the immune system, macrophages play an important role in angiogenesis and bone regeneration during bone repair<sup>[6-8]</sup>. The phenotypic transition of macrophages is dynamic and plastic, and can be divided into M1 and M2 macrophages according to the immune response of the surrounding microenvironment<sup>[9,10]</sup>. Classical M1 macrophages are generally considered pro-inflammatory cells that secrete tumor necrosis factor (TNF)- $\alpha$  and interleukin (IL)-1 $\beta$  cytokines to accelerate the progression of inflammation. M2 macrophages are considered anti-inflammatory cells that release tissue repair factors, such as TNF- $\beta$ , bone morphogenetic protein-2 (BMP-2), vascular endothelial growth factor (VEGF), and platelet-derived growth factor BB (PDGF-bb), which can promote vascularization, osteogenic differentiation, and tissue repair<sup>[11-13]</sup>. In recent years, several studies have used bone repair materials to load ions and cytokines with immunomodulatory effects to achieve the regulation of macrophage phenotype polarization and promote the osteogenic differentiation of stem cells and the healing of bone defects, which further confirms the role of macrophages in bone defect repair<sup>[14-16]</sup>. Therefore, bone repair materials with immunomodulatory effects should have the effect of inducing phenotypic polarization of macrophages, thereby establishing a microenvironment that enhances osteogenesis.

Studies have shown that the pore structure of materials plays an indispensable role in regulating the polarization phenotype of macrophages. Garg *et al.* found that increasing the pore size of electrospun scaffolds from 1.92 to 29.46  $\mu\text{m}$  induces polarization of macrophages toward the M2 phenotype<sup>[17]</sup>. Luu *et al.* found that the morphology and polarization state of macrophages can be changed by using the surface topology changes of materials, and the micro-nano grooves can promote the growth of macrophages and the polarization of macrophages to M2 phenotype<sup>[18]</sup>. The scaffold pore size can affect the polarization phenotype of macrophages, and scaffolds with large pore sizes showed greater potential in promoting M1-to-M2-type polarization<sup>[18]</sup>. Sussman *et al.* found that macrophages in scaffolds with an average pore size of 160  $\mu\text{m}$  tended to express higher levels of the M2 marker compared to scaffolds with an average pore size of 34  $\mu\text{m}$ <sup>[19]</sup>. Previous studies have shown that the phenotypic polarization of macrophages is sensitive to the pore size of the material, so it is feasible to modulate the phenotype of macrophages by designing the pore size of the material.

Poly(ether-ether-ketone) (PEEK), as a semi-crystalline, non-absorbable thermoplastic material with stable chemical properties, excellent mechanical properties, and low friction properties, is considered one of the most promising orthopedic implant materials<sup>[20-22]</sup>. However, as an “inert” material, the poor biocompatibility and osseointegration properties of PEEK limit its wide clinical application<sup>[15,23-25]</sup>. Based on the sensitivity of phenotypic polarization of macrophages to material pore size and the role of macrophages in mediating osseointegration, we believe that regulating macrophage polarization by changing the pore size of PEEK scaffold can enhance bone integration between PEEK scaffold and host bone, and finally promote the rapid repair of bone defects. To test this hypothesis, we constructed three-dimensional (3D)-printed PEEK scaffolds with pore sizes of 0, 200, and 400  $\mu\text{m}$ , and used *in vitro* and *in vivo* experiments to investigate the effect of scaffold pore size on macrophage polarization and subsequent angiogenesis and osteogenesis. The macrophage response to PEEK scaffold pore size and the potential relationship between scaffold pore size, macrophage function, and osseointegration were further explored, hoping to provide new insights into promoting osseointegration of PEEK bone repair materials.

## 2. Material and methods

### 2.1. Preparation of 3D-printed PEEK scaffolds

Powdered medical PEEK raw materials were prepared into filaments with a diameter of 1.75 mm, and then PEEK scaffolds (printing temperature = 420°C, nozzle diameter = 400  $\mu\text{m}$ , layer height = 400  $\mu\text{m}$ , scaffold diameter = 8 mm, scaffold thickness = 3 or 10 mm) with different pore sizes were printed by FDM 3D printer (JUGAO-AM, Surgeon Plus, China), and the scaffolds with pore sizes of 0, 200, and 400  $\mu\text{m}$  were named PEEK0, PEEK200, and PEEK400, respectively. In order to increase the hydrophilicity of PEEK scaffolds, the PEEK scaffolds were washed in deionized water, ethanol, and acetone in turn, and then the PEEK scaffolds were immersed in concentrated sulfuric acid for 15 s, and then immersed in concentrated nitric acid at 70°C for 30 min<sup>[15,26]</sup>. After ultrasonic cleaning (three times, 20 min each time), the samples were soaked in deionized water for 24 h to remove excess acid, and finally 3D-printed hydrophilized-PEEK scaffolds with different pore sizes were obtained.

### 2.2. Characterization of 3D-printed PEEK scaffolds

#### 2.2.1. Scanning electron microscopy (SEM)

All samples were sputter-coated with an Ion Sputter (E-1010, Hitachi, Tokyo, Japan), and the morphology was observed by scanning electron microscope (SEM, S2400, Hitachi).

### 2.2.2. Water contact angle

The water contact angle of the untreated, sulfuric acid-treated and nitric acid-treated scaffold was measured by using a Drop Shape Analysis System DSA100 (Kruss, Germany) at room temperature.

### 2.2.3. Parameters of scaffold pore

According to the SEM image of the scaffold, the distance (pore size) between the printed filaments in the SEM image of the scaffold was counted using ImageJ software, and the average value of 20 pore sizes was counted and calculated. According to the pore size measured by SEM and the width of the printing wire, the average porosity of five scaffolds was calculated. The connectivity between the pores of the scaffold was observed, and the pore connectivity of the 20 scaffolds was counted and calculated.

## 2.3. Characteristics of macrophages incubated in 3D-printed PEEK scaffolds

### 2.3.1. Macrophage seeding

RAW264.7 (murine monocyte/macrophage cell line) were obtained from American Type Culture Collection (ATCC) and incubated in basal culture media composed of Dulbecco's modified eagle medium (DMEM; Gibco) supplemented with 10% fetal bovine serum (FBS; Gibco) and 1% penicillin and streptomycin (HyClone) in 25 cm<sup>2</sup> culture flask. The induction of M1 macrophages followed the steps below after RAW264.7 cells were adherently cultured in culture flasks overnight, and the medium was changed to induction medium containing 20 ng/mL interferon gamma (IFN- $\gamma$ ) and 100 ng/mL lipopolysaccharide (LPS). After induction culture for 12 h, the induction medium was replaced with complete medium, and M1 macrophages were obtained after culturing for 24 h.

For cell seeding, 3D-printed PEEK scaffolds (10 mm in diameter, 3 mm in height) were sterilized and pre-incubated with DMEM for 12 h. Subsequently, the M1 macrophages were washed three times with phosphate-buffered saline (PBS), and then the concentrated suspensions of macrophage were injected evenly on the surface of the PEEK scaffold. The scaffolds were cultured in a humidified atmosphere of 5% CO<sub>2</sub>, 37 °C for 1 h, and basal culture media were added for further incubation; the medium was changed every 2 days.

### 2.3.2. Macrophage proliferation and adhesion on scaffolds

M1 macrophages were seeded on the surface of PEEK0, PEEK200, and PEEK400 scaffolds at a density of  $2 \times 10^4$  cells/well and then cultured for a further 1, 4, and 7 days. Then, the original medium was removed, CCK-8 working solution (a mixture of 90% complete medium and 10% CCK-8) was added and incubated at 37°C, 5%

CO<sub>2</sub> for 30 min, and then, a microplate reader (BIO-RAD 680, USA) was used to test the absorbance value (OD<sub>450</sub>) of the culture solution at 450 nm. The adhesion and distribution of macrophages on the surface of PEEK scaffolds were observed by fluorescence microscope. After macrophage seeding for 7 days, the cells were fixed in 4% paraformaldehyde for 30 min. All samples were rinsed several times with PBS and permeabilized with 0.5% Triton X-100. After that, cells were stained with 70 nM FITC-labeled rhodamine phalloidin (Solarbio, China), washed with PBS after incubation for 30 min. The fluorescence images of the constructs were observed with a confocal microscope (LSM880, Zeiss, Germany).

### 2.3.3. Cytokine measurements

M1 macrophages were seeded on the surface of PEEK0, PEEK200, and PEEK400 scaffolds at a density of  $2 \times 10^4$  cells/well, and the supernatant of each experimental group was collected after 3 days of incubation. The concentrations of TNF- $\alpha$ , IL-6, IL-10, BMP-2, VEGF, and PDGF-bb were quantified by ELISA kit (4A Biotech).

### 2.3.4. Expression of macrophage polarization-related genes

To simulate the state of acute inflammatory response produced by biomaterials in the early stage of implantation, M1 macrophages were seeded on the surface of 3D-printed PEEK scaffolds with different pore sizes at a density of  $1 \times 10^5$  cells/well. After 3 days of co-culture, the cells were collected and washed with PBS for three times. Total RNA was isolated using the Trizol Reagent (Life Technologies, USA) method as described by the manufacturer (BIO-RAD 680, USA). cDNA was synthesized from the isolated RNA using PrimeScript™ cDNA synthesis kit (TaKaRa Bio, Japan). The sequences of forward and reverse primers of housekeeping gene and target gene (C-C chemokine receptor type 7 [CCR7], TNF- $\alpha$ , inducible nitric oxide synthase [iNOS], VEGF, CD206, TGF- $\beta$ , BMP-2, and PDGF-bb) are listed in **Table S1** (Supplementary File). RT-PCR samples were prepared by mixing the cDNA, SYBR Green qPCR Master Mix (Life Technologies), and the primers, and the RT-qPCR was performed utilizing the 7500HT Fast Real-Time PCR (Applied Biosystems, USA). The relative gene expression was calculated using the  $2^{-\Delta\Delta Ct}$  method with *GAPDH* as the reference gene.

## 2.4. Paracrine effect of macrophage on BMSCs

### 2.4.1. Preparation of macrophage-conditioned media

Conditioned medium (CM) is the supernatant of the medium produced after co-culture of macrophages and scaffolds<sup>[27]</sup>. After the scaffolds were co-cultured with macrophages for 3 days, the supernatant was collected, centrifuged at 300×g for 1 h to remove any residual, and then filter-sterilized using a 0.22- $\mu$ m sterile microporous

filter, and CM of scaffolds with different pore sizes was finally obtained.

#### 2.4.2. BMSCs growth and adhesion

BMSCs were seeded at a density of  $3 \times 10^4$  cells/well and cultured in the CM for 48 h and then cultured for a further 3 and 7 days in osteogenic media (DMEM supplemented with  $10^{-7}$  M dexamethasone,  $10^{-2}$  M  $\beta$ -Glycerophosphate, and 50  $\mu$ g/mL ascorbic acid [Sigma, USA])<sup>[28]</sup>. Then, the original medium was removed, and CCK-8 working solution (a mixture of 90% complete medium and 10% CCK-8) was added and incubated at 37°C, 5% CO<sub>2</sub> for 30 min. One hundred microliter of the incubated culture solution was transferred to a 96-well plate, and a microplate reader (BIO-RAD 680, USA) was used to test the absorbance value (OD<sub>450</sub>) of the culture solution at 450 nm.

The adhesion and distribution of BMSCs on the surface of PEEK scaffolds were observed by fluorescence microscope. After BMSCs seeding for 7 days, the cells were fixed in 4% paraformaldehyde for 30 min. All samples were rinsed several times with PBS and permeabilized with 0.5% Triton X-100. After that, cells were stained with 70 nM FITC-labeled rhodamine phalloidin (Solarbio, China), washed with PBS after 30 min of incubation. The fluorescence images of the constructs were observed with a confocal microscope (LSM880, Zeiss, Germany).

#### 2.4.3. Expression of osteogenesis-related genes

BMSCs were seeded at a density of  $3 \times 10^4$  cells/well and cultured in the basal culture media or CM for 48 h and then cultured for a further 7 days in osteogenic media. After 7 days of culture, the cells were collected and washed with PBS for 3 times. RT-PCR was used to detect the expression of osteogenesis-related genes, and the detection steps were the same as those in Section 2.3.4. The sequences of forward and reverse primers of target genes (*ALP*, *OCN*, *OPN*, and *RUNX2*) are listed in **Table S2** (Supplementary File).

#### 2.4.4. ALP activity analysis

BMSCs were seeded at a density of  $3 \times 10^4$  cells/well and cultured in the basal culture media or CM for 48 h and then cultured for a further 7 and 14 days in osteogenic media. According to the instructions of the kit, ALP assay kit (Solarbio, China) and BCA Protein assay kit (Solarbio, China) were used to determine the ALP activity of BMSCs, and three independent experiments were conducted.

#### 2.4.5. Alizarin red S staining

BMSCs were seeded at a density of  $3 \times 10^4$  cells/well and cultured in the basal culture media or CM for 48 h and then cultured for a further 21 days in osteogenic media. After 21 days of culture, the supernatants were removed, and cells were rinsed with PBS for 3 times. Then, the cells

were incubated in 40 mM Alizarin red S for 10 min after being fixed with 4% paraformaldehyde for 30 min. The cell mineralization was observed by using stereomicroscope (SteREO, ZEISS, Germany). The optical density (OD) value was measured at 540 nm after the stain was solubilized with 10% cetylpyridinium chloride.

### 2.5. Paracrine effect of macrophage on HUVECs

#### 2.5.1. Scratch healing experiment

HUVECs were seeded in 6-well plates at a density of  $1 \times 10^5$  cells/well and incubated overnight. When cells reached 90% confluency, a sterile 200- $\mu$ L pipette tip was used to make a cell-free scratch in the middle of the monolayer of HUVECs and rinsed with PBS to remove unadhered cells as well as cell fragments<sup>[29]</sup>. Furthermore, after adding different CMs, HUVECs were further cultured at 37°C and 5% CO<sub>2</sub> for 12 and 24 h. After 0, 12, and 24 h of incubation, the scratches were photographed with a microscope, and then the scratch area was quantitatively analyzed using ImageJ software, and the scratch healing rate was calculated using Equation 1:

$$\text{Wound area (\%)} = \frac{A_t}{A_0} \times 100\% \quad (1)$$

where  $A_t$  is the area of scratches at different time points, and  $A_0$  is the area of scratches at 0 h.

#### 2.5.2. Expression of angiogenesis-related genes

HUVECs cells were seeded in 24-well plates at a density of  $1 \times 10^5$  cells/well and cultured overnight, and then, the cell culture medium was changed to a 1:1 mixed medium of CM and complete medium. After 3 days of co-culture, the cells were collected and washed with PBS for 3 times. RT-PCR was used to detect the expression of angiogenesis-related genes, and the detection steps were the same as those in section 2.3.3. The sequences of forward and reverse primers of target genes (*Angiogenin*, *FGF*, and *SDF*) are listed in **Table S3** (Supplementary File).

### 2.6. Animal experiment

#### 2.6.1. Surgical procedure

Ethical approval was obtained from the Experimental Animal Ethics Committee of Jinan University. The tibial defect model animals used were New Zealand rabbits, which were purchased from Huadong Xinhua Experimental Animal Farm. Then, the rabbits were anesthetized with 3% sodium pentobarbital (1 mL/kg) and xylazine hydrochloride (0.1 mL/kg), and the hind limbs of rabbits were cleaned and disinfected with iodophor and alcohol. Afterward, a defect of 8 mm in diameter and 3 mm in depth was made on the tibial plateau with a trephine with a diameter of 8 mm, and then the sterilized 3D-printed PEEK scaffold was implanted into the defect. Then, the wound was sutured layer by layer, and the rabbits

were allowed to recover. On dates of scheduled explant retrieval, rats were sacrificed by CO<sub>2</sub> asphyxiation. The repaired femur, with the PEEK plate fixator intact, was carefully separated from the adjacent hip and knee joints for analysis.

### 2.6.2. In vitro micro-CT analysis

After 4, 8, and 12 weeks of implantation, the rabbits were killed by excessive injection of chloral hydrate anesthesia, and the specimens were obtained and fixed in 10% formaldehyde solution. The specimens were scanned at a pixel size of 30 μm using a micro-CT (SkyScan 1176, Bruker, Germany), and the 3D structure was reconstructed from the acquired two-dimensional (2D) continuous tomographic images. The region of interest (ROI) was accurately located according to the 3D image to ensure that the bone defect, scaffold, and new bone can be fully covered. After the new bone and residual scaffold in the ROI region was distinguished, the bone volume/total volume ratio (BV/TV), bone surface/bone volume (BS/BV), trabecular thickness (Tb.Th), and trabecular Number (Tb.N) at different implantation time points were systematically analyzed.

### 2.6.3. Histological staining

After micro-CT scanning, the specimens were dehydrated and embedded in polymethyl methacrylate. Then, the specimens were serially sectioned at a thickness of 5 μm and placed on the glass slide. The sections were stained with hematoxylin & eosin (H&E), Masson's trichrome, and von Kossa to assess the bone surrounding the scaffold, and then observed under a light microscope (ZEISS, Germany).

### 2.6.4. Biomechanical analysis

A biomechanical testing machine (Electro Force 3510, USA) was used to test the bonding strength between the PEEK scaffold and the host bone. The compression rate was 2 mm/min, and the maximum load force and stiffness were calculated.

### 2.7. Statistical analysis

All statistical analyses were carried out by using SPSS version 10.1 software (SPSS Inc., USA). Statistically significant differences ( $p < 0.05$ ) between the various groups were adjusted using the Tukey-Kramer *post-hoc* test. All the data are expressed as means ± standard deviation (SD).

## 3. Results

### 3.1. Characteristics of 3D-printed PEEK scaffolds

The macro- and micro-morphologies of 3D-printed PEEK scaffolds with different pore sizes are shown in Figure 1A. It can be seen that the structure of the prepared PEEK

scaffold is relatively regular, which can also be proven by the SEM results. The SEM results also show that the diameter of the printing wire of PEEK scaffold is relatively uniform, and no broken wire and defects are found. To improve the hydrophilicity of the 3D-printed PEEK scaffolds, the PEEK scaffolds were treated with concentrated sulfuric acid and concentrated nitric acid in turn, and the contact angle and microstructure before and after the treatment were tested, as shown in Figure 1B. The contact angle of PEEK scaffolds treated with concentrated sulfuric acid and concentrated nitric acid decreased from 90° to 65°, and the hydrophilicity was significantly improved. In addition, SEM results showed that the surface of the acid-treated scaffolds formed a uniformly distributed layered porous structure with a pore size of about 1–2 μm.

In addition, based on the SEM results of the scaffolds, the pore size, porosity, and pore connectivity of the 3D-printed PEEK scaffolds were analyzed, as shown in Table 1. The actual pore size obtained by measurement and statistics is basically consistent with the preset pore size, and the porosity of the scaffold gradually increases with the increase of the pore size. However, the connectivity rates of scaffolds with different pore sizes are all around 100%, which indicates that scaffolds with different pore sizes all have good 3D connectivity structures. The results of the study of mechanical properties showed that the compressive strength of the scaffold gradually decreases with the increase of the pore size (Figure S1 in Supplementary File). In addition, the results of proliferation and fluorescent staining of L929 cells on the 3D-printed scaffold group showed that the 3D-printed PEEK scaffolds with different pore sizes had good biocompatibility (Figure S2 in Supplementary File).

### 3.2. In vitro macrophage polarization

The proliferation results (Figure 2A) of macrophages co-cultured with the scaffold for 1, 4, and 7 days showed that there was no significant difference in the number of cells in the scaffold groups with different pore sizes, which indicated that the pore size of the scaffold had no effect on cell proliferation. Fluorescence staining results (Figure 2B) after 7 days of cell culture showed that macrophages grew well on the scaffold surface, and there was no significant difference between different groups, which was consistent with the cell proliferation results.

The expression of polarization-related genes in macrophages was detected by RT-PCR, as shown in Figure 3A. Compared with the PEEK group, the expression levels of the M1 macrophage-related genes *iNOS* and nuclear factor kappa B (*NF-κB*) in the PEEK400 group were relatively lower, while the expression levels of the M2 macrophage-related genes *CD206*, *TGF-β*, and *IL-*

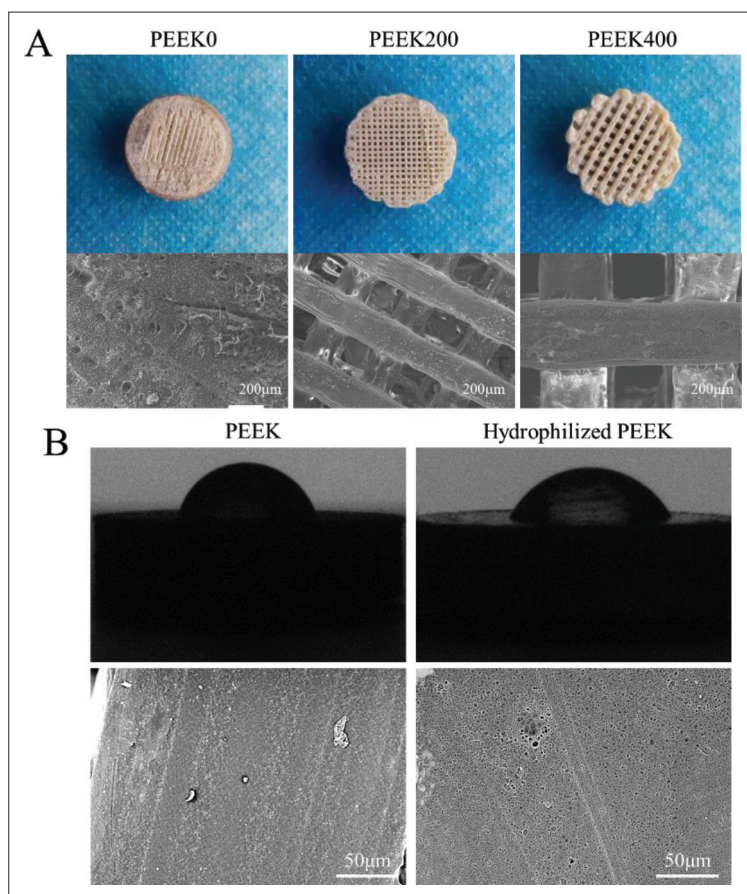


**Figure 1.** Characterization of PEEK and hydrophilized PEEK scaffold. (A) General morphology and SEM image of 3D-printed PEEK scaffold with different pore size (0, 200, and 400  $\mu\text{m}$ ). (B) Water contact angle and surface morphologies of PEEK and hydrophilized PEEK.

**Table 1.** Pore parameters of 3D-printed PEEK scaffolds.

	Preset pore ( $\mu\text{m}$ ) size/ $\mu\text{m}$	Actual pore size ( $\mu\text{m}$ )	Porosity (%)	Pore connectivity (%)
PEEK0	0	/	/	/
PEEK200	200	204.03 $\pm$ 10.03	45.54 $\pm$ 2.97	99.7 $\pm$ 0.49
PEEK400	400	381.92 $\pm$ 17.66	62.77 $\pm$ 4.26	100 $\pm$ 0.24

10 were significantly higher ( $p < 0.05$ ). In addition, the results of flow cytometry showed that the expression of *CD86* decreased with the increase of pore size, while the expression of *CD206* increased with the increase of pore size (Figure S3 in Supplementary File). The results of macrophage phenotype polarization indicated that macrophages were responsive to the pore size of 3D-printed PEEK scaffolds, and scaffolds with larger pore sizes could induce macrophages to switch from M1 to M2 type.

Macrophages release a large amount of cytokines in the process of recognizing material properties and polarizing into different phenotypes, and then perform different functions. The secretion of inflammation-related

factors, anti-inflammatory factors, and pro-osteogenic and pro-angiogenesis-related factors was detected by ELISA after macrophages were cultured on the surface of the samples for 4 days, as shown in Figure 3B. Similar to the PCR results, there was no significant difference in the release of macrophage pro-inflammatory factors IL-6 and TNF- $\alpha$  between different groups, while the release of anti-inflammatory factors TGF- $\beta$  and IL-10 in the PEEK400 scaffold group was significantly higher than that in the PEEK group. In addition, the PEEK400 scaffold group had the highest release of the pro-osteogenic factor BMP-2 and the angiogenesis-related factor PDGF-bb. The pore size of the scaffold has no effect on the degree of inflammatory response of macrophages, but the scaffold with larger

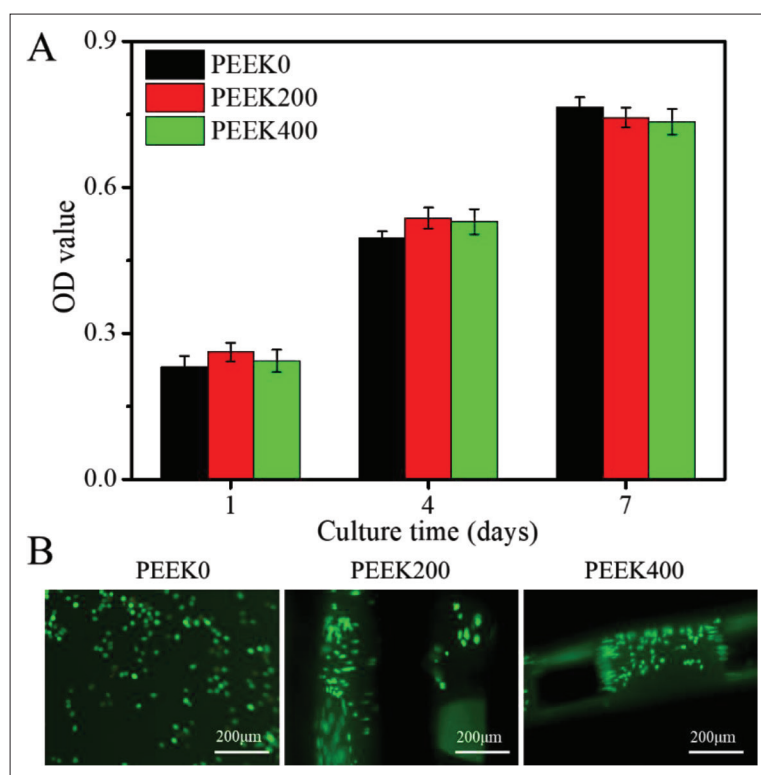


**Figure 2.** Proliferation and adhesion of cells on PEEK scaffolds with different pore sizes. (A) CCK-8 results of M1 macrophage cultured on PEEK scaffold with different pore sizes (0, 200, and 400  $\mu\text{m}$ ) for 1, 4, and 7 days. (B) The fluorescence staining of macrophages co-cultured with scaffolds of different pore sizes for 7 days (scale bar = 200  $\mu\text{m}$ ).

pore size can promote the anti-inflammatory effect of macrophages and increase the release of osteogenesis and angiogenesis-related factors.

### 3.3. Macrophage-mediated osteogenic activity

To evaluate the immunomodulatory effect of samples, the supernatants from macrophage cultures were used as CM to evaluate the osteogenic activity of BMSCs. The time-based proliferation of BMSCs is shown in Figure 4. After incubation for 1 day, no obvious difference was reported among the three groups. The PEEK200 and the PEEK400 showed higher proliferation rate in comparison with the PEEK after 4 and 7 days of culture, and the rabbit BMSCs exhibited much greater proliferation on the PEEK400 group ( $p < 0.01$ ). Figure 4B showed the cell morphology of rabbit BMSCs cultured for 7 days. It can be seen that the cells in the PEEK group grow mono-dispersedly, while the cells in the PEEK400 group are connected to each other and spread more obviously, indicating that the paracrine secretions after co-culture of macrophages with macropore-sized scaffolds can promote the proliferation and adhesion of BMSCs, which is consistent with the results of CCK-8.

ALP is one of the commonly used indicators for the osteogenic differentiation of BMSCs. To examine the

direct effect of paracrine secretions after co-culture of macrophages with scaffolds on the induction of osteogenic differentiation of BMSCs, the ALP activity of BMSCs after 14 days of culture in CM was examined, as shown in Figure 5B. The results showed that the ALP activity in the PEEK group was relatively the lowest, while the ALP activity in the PEEK400 group was the highest, and there was a statistical difference between the two groups. The results of ALP staining (Figure 5A) showed that the ALP staining in the PEEK200 and PEEK400 scaffold groups was significantly deeper than that in the PEEK group after BMSCs were induced and cultured for 14 days, and the PEEK400 group had the most obvious staining results, which reconfirmed the results of ALP. Furthermore, the Alizarin red S staining results (Figure 5D) showed that with the increase of pore size, the staining of Alizarin red S gradually became intense, and the semi-quantitative results of Alizarin red S staining (Figure 5C) showed that the OD value at 600 nm of the PEEK400 scaffold group was significantly higher. This indicates that the paracrine secretion of macrophages in PEEK400 group induces a higher level of extracellular mineralization of BMSCs, which also means that it has the strongest effect on inducing osteogenic differentiation, which can be mutually confirmed with the results of ALP activity.

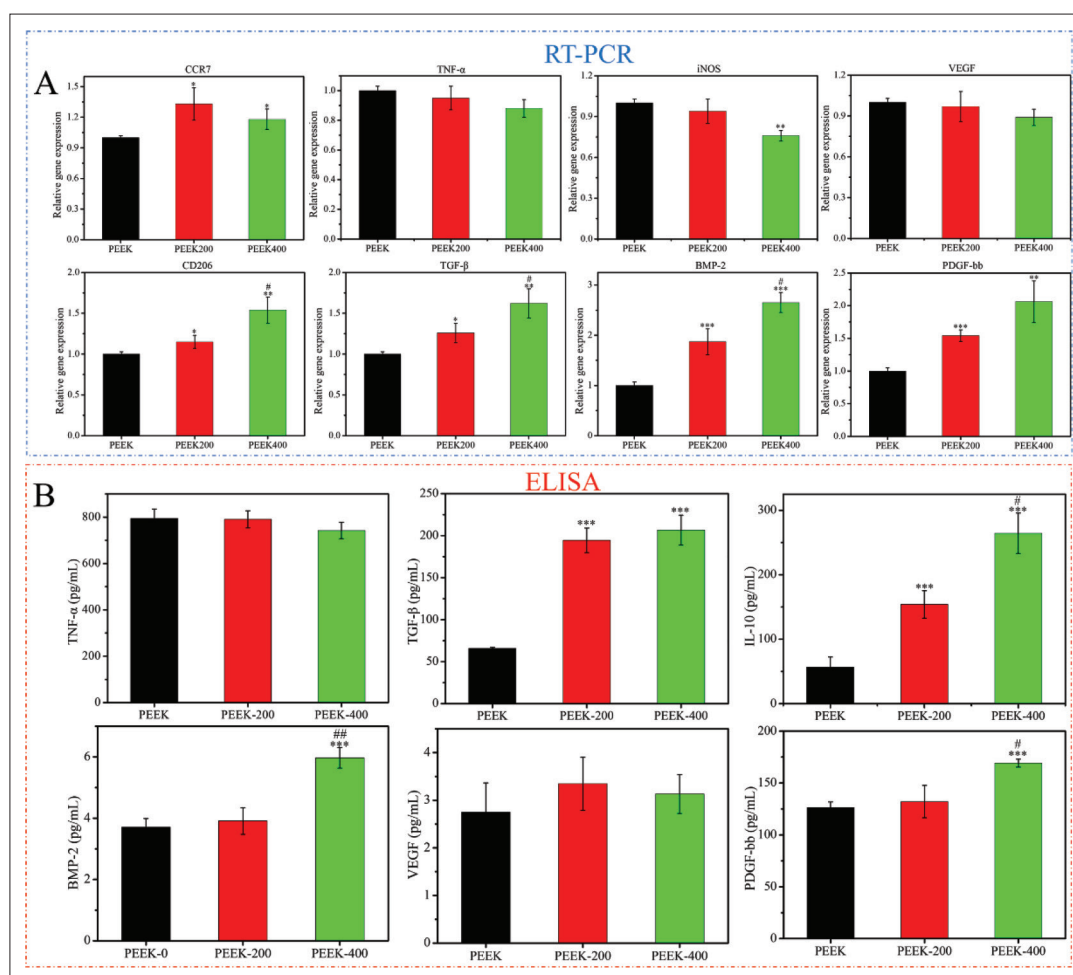


**Figure 3.** Macrophage polarization-related gene expression and cytokines levels in the supernatants determined by RT-qPCR and ELISA after macrophage co-cultured with PEEK scaffold for 3 days. (A) mRNA level of *CCR7*, *TNF- $\alpha$* , *iNOS*, *VEGF*, *CD206*, *TGF- $\beta$* , *BMP-2*, and *PDGF-bb*. (B) ELISA results of cytokines of *TNF- $\alpha$* , *TGF- $\beta$* , *IL-10*, *BMP-2*, *VEGF*, and *PDGF-bb*. Data are expressed as the mean  $\pm$  SD for  $n \geq 3$ ; \* $p < 0.05$ , \*\* $p < 0.01$ , and \*\*\* $p < 0.001$  indicate significant differences when compared to the PEEK0; # $p < 0.05$ , ## $p < 0.01$ , and ### $p < 0.001$  indicate significant differences when compared to the PEEK200.

The expression levels of osteogenic genes (*ALP*, *OCN*, *OPN*, and *RUNX2*) in BMSCs were detected by RT-qPCR, as shown in Figure 5E. The results showed that the expressions of *ALP*, *OCN*, and *RUNX2* genes in BMSCs in PEEK400 scaffold group and PEEK200 group were significantly higher than those in PEEK0 group, and there were statistical differences between the groups. At the same time, the gene expression of *ALP* and *RUNX2* was also statistically different between the PEEK200 and PEEK400 groups. The results of RT-qPCR indicated that paracrine secretions after co-culture of macrophages with macropore-sized PEEK scaffolds could mediate the high expression of osteogenic genes in BMSCs.

### 3.4. Macrophage-mediated angiogenic properties

The response of HUVECs to paracrine secretion after co-culture of macrophages and scaffolds was explored by

scratch healing experiments, as shown in Figure 6. After 12 and 24 h of culture, HUVECs in each group gradually migrated to the center (Figure 6A), while the migration of HUVECs in PEEK400 group was more obvious. In addition, the quantitative results of the scratch area showed that the scratch area of the PEEK400 scaffold group was significantly reduced compared with the PEEK group (Figure 6B), which explained the conditioned medium after the co-culture of macrophages with the PEEK0 scaffold. It can promote the migration of HUVECs, thereby promoting the healing of scratches. Figure 6C shows the expressions of angiogenesis-related genes (*Angiogenin*, *FGF-2*, and *SDF*) after culturing HUVECs in a 1:1 mixture of CM and complete medium for 3 days. The expressions of *Angiogenin* and *SDF* genes in PEEK200 and PEEK400 groups were significantly upregulated compared with



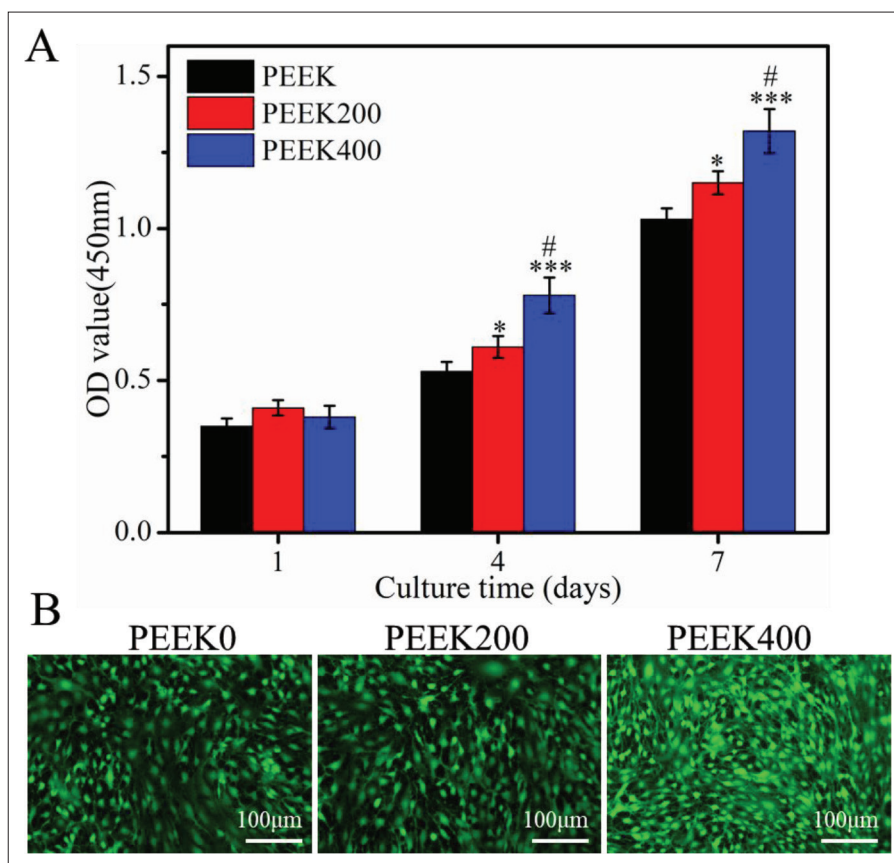


**Figure 4.** *In vitro* proliferation assessment of BMSCs cultured in macrophage-conditioned medium for 1, 4, and 7 days. Conditioned medium is the supernatant of the medium produced after co-culture of macrophages and scaffolds for 3 days. (A) CCK-8 results of BMSCs cultured in various conditioned medium for 1, 4, and 7 days. Data are shown as the mean  $\pm$  SD for  $n \geq 3$ ; \* $p < 0.05$ , \*\* $p < 0.01$ , and \*\*\* $p < 0.001$  indicate significant differences when compared to the PEEK0; # $p < 0.05$  indicates significant differences when compared to the PEEK200. (B) Fluorescent staining of BMSCs cultured in conditioned medium for 7 days (scale bar = 100  $\mu$ m).

PEEK0 group ( $p < 0.05$ ), and there was also a significant difference between PEEK400 and PEEK200 groups. The above results indicated that the CM after co-culture of macrophages with large-pore PEEK scaffolds had a significant effect on promoting angiogenesis *in vitro*.

### 3.5. *In vivo* animal experiments

To verify the osseointegration effect of 3D-printed PEEK scaffolds with different pore sizes, the scaffolds were implanted into the tibia defect of rabbits. The results of 3D reconstruction and sagittal and coronal images (Figure 7A) after 12 weeks of implantation showed that the PEEK scaffold only had a small amount of new bone formation on the surface of the scaffold, and there was no new bone formation at the edge. New bone was formed at the interface between scaffold the PEEK200 scaffold and the host bone, and grew into the interior of the scaffold. However, the new bone formation in the PEEK400 scaffold group was more obvious, and it could be observed that the new bone grew into the inside of the scaffold and

the shape of the new bone matched the pore structure of the PEEK400 scaffold. The results of animal experiments showed that scaffolds with large pore size significantly generated new bone, and the 3D images of the ROI area also proved this result.

To further verify the results of micro-CT scans, BV/TV, BS/BV, Tb.Th, and Tb.N osteogenesis-related indicators were analyzed by CTAn (SkyScan, Bruker micro CT, Germany) software, as shown in Figure 7B. The results showed that the BV/TV, Tb.Th, and Tb.N indexes of the PEEK400 scaffold group were the highest, while the BS/BV indexes were the lowest, and it was statistically significant compared with other groups, indicating that the amount of new bone formed in the PEEK400 scaffold group was higher than that in the other groups.

Furthermore, H&E, Masson's trichrome, and von Kossa staining were performed to stain the newly developed bone tissue, cartilage tissue, and calcium deposition, as shown in Figure 8. It can be seen that in the PEEK0 scaffold

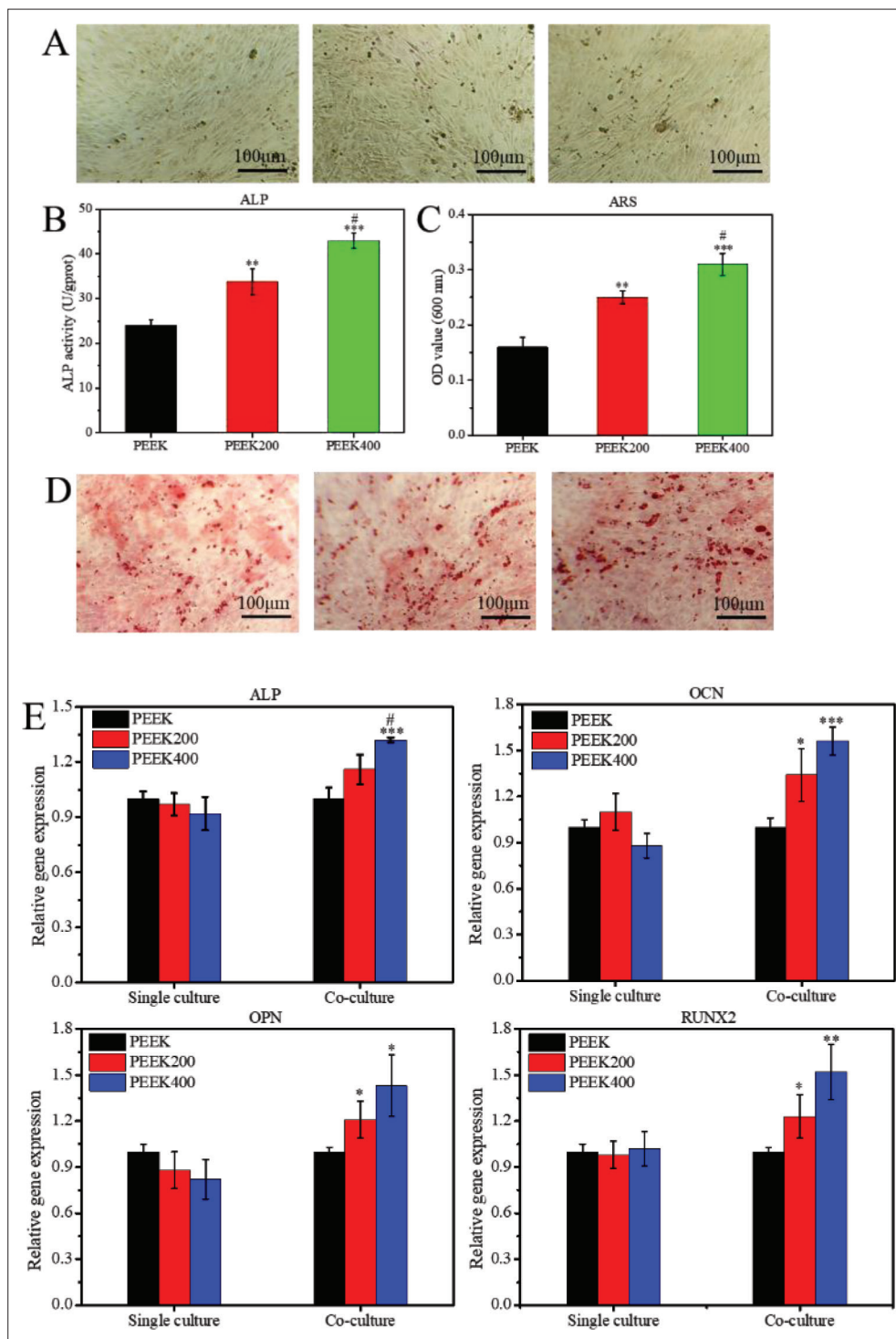


**Figure 5.** *In vitro* osteogenic differentiation evaluation of the macrophage-conditioned medium. Conditioned medium is the supernatant of the medium produced after co-culture of macrophages and scaffolds for 3 days. (A) ALP staining of BMSCs cultured in conditioned medium for 14 days (scale bar = 100  $\mu$ m). (B and C) Quantitative analysis of ALP staining and Alizarin red S staining, respectively. (D) Alizarin red S staining of BMSCs cultured in conditioned medium for 14 days (scale bar = 100  $\mu$ m). (E) Expression of osteogenesis-related genes (*ALP*, *OCN*, *OPN*, and *RUNX2*) of rabbit BMSCs cultured in conditioned medium at day 14. Data are shown as the mean  $\pm$  SD for  $n \geq 3$ ; \* $p < 0.05$ , \*\* $p < 0.01$ , and \*\*\* $p < 0.001$  indicate significant differences when compared to the PEEK0; \* $p < 0.05$  indicates significant differences when compared to the PEEK200.

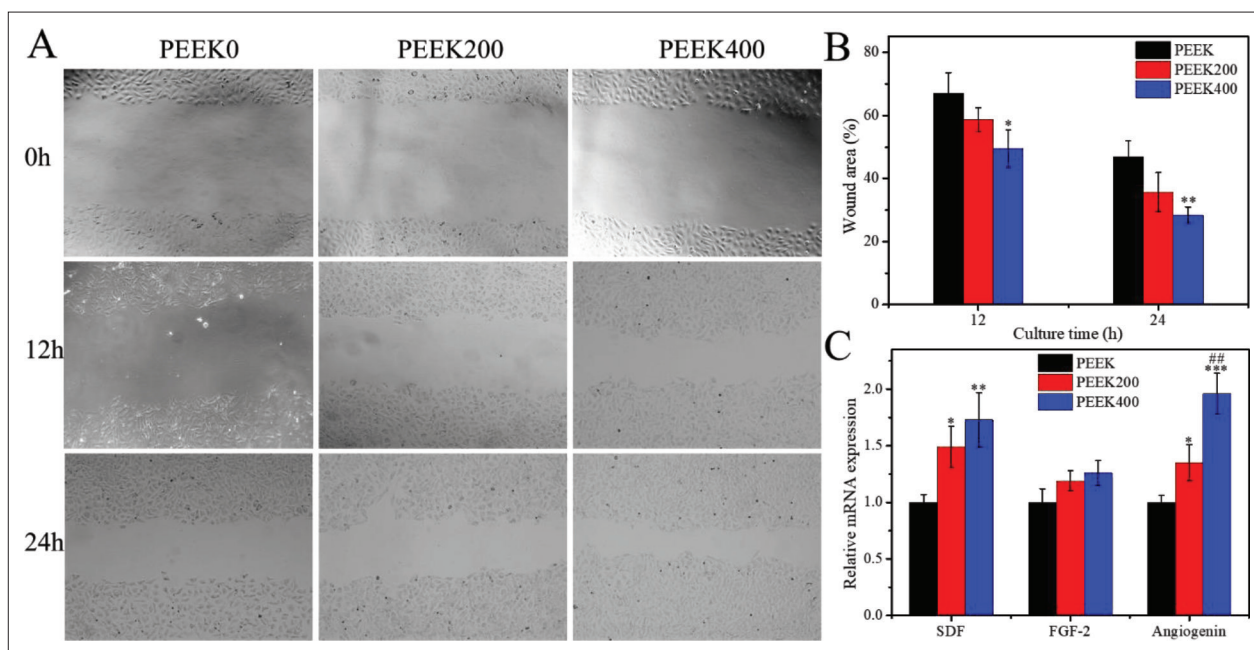


**Figure 6.** Effects of conditioned medium on *in vitro* HUVECs migration and angiogenesis-related gene expression. Conditioned medium is the supernatant of the medium produced after co-culture of macrophages and scaffolds for 3 days. (A) Representative images showing HUVECs migration (scratch assay) after cell cultivation in conditioned medium for 0 (baseline), 12, and 24 h. (B) Quantitative analysis of the scratch confluence of migrated cells following cell cultivation in conditioned medium for 12 and 24 h. (C) Expression of angiogenesis-related genes (*Angiogenin*, *FGF-2*, and *SDF*) in HUVECs cultured in conditioned medium for 3 days. Data are shown as the mean  $\pm$  SD for  $n \geq 3$ ; \* $p < 0.05$ , \*\* $p < 0.01$ , and \*\*\* $p < 0.001$  indicate significant differences when compared to the PEEK0; \* $p < 0.05$ , \*\* $p < 0.01$ , and \*\*\* $p < 0.001$  indicate significant differences when compared to the PEEK200.

group, only PEEK scaffolds can be seen in the defect area, and no new bone tissue, cartilage tissue, and calcium salt deposition were found. For PEEK200 scaffold, new bone matrix and cartilage tissue transformed into bone tissue, which was embedded at the edge of the scaffold, and calcium deposition also appeared in the scaffold, indicating that bone integration has occurred between the PEEK200 scaffold and the host bone. For the PEEK400 scaffold, more new bone matrix and cartilage tissue appeared in the scaffold, and the results of von Kossa staining showed that the calcium salt deposition degree inside the scaffold was similar to that in the host bone, which may suggest that there is a greater amount of new and more mature bone in the PEEK400 scaffold. The results of histological staining showed that the scaffold with large pore size could promote the growth of new bone, thereby enhancing the integration of bone and scaffold interface.

Biomechanical properties are a key indicator for evaluating the osseointegration of materials with host bone. To examine the osseointegration properties of 3D-printed PEEK scaffolds with different pore sizes, biomechanical tests were performed on the specimens after 12 weeks of implantation, as shown in Figure 9. The results showed that the maximum load and stiffness gradually increased with the increase of pore size, and the PEEK400 group

had a significant difference compared with other groups, which indicated that the PEEK400 scaffold had the best osseointegration ability and biomechanical properties.

#### 4. Discussion

The host immune response is an important factor affecting the fate of bone repair materials, and previous studies have minimized the host immune response to improve the effect of implantation<sup>[30,31]</sup>. However, it is now generally believed that the immune system has a positive effect on bone regeneration, and the responses generated by immune cells not only produce foreign body responses to bone repair materials, but also participate in and mediate the process of angiogenesis and osteogenesis<sup>[12,32-34]</sup>. As core cells of the bone immune system, diversity, and plasticity are typical of macrophages, their ability to alter phenotype through subtle changes in the microenvironment has been widely described. The polarization of macrophages to different phenotypes may have different functions, which in turn trigger completely different effects on bone repair. Thus, favorable macrophage phenotypic polarization modulated by bone repair materials will ensure vascularization of the material and integration of the material with host bone. The importance of pore size on bone repair materials for angiogenesis and new bone

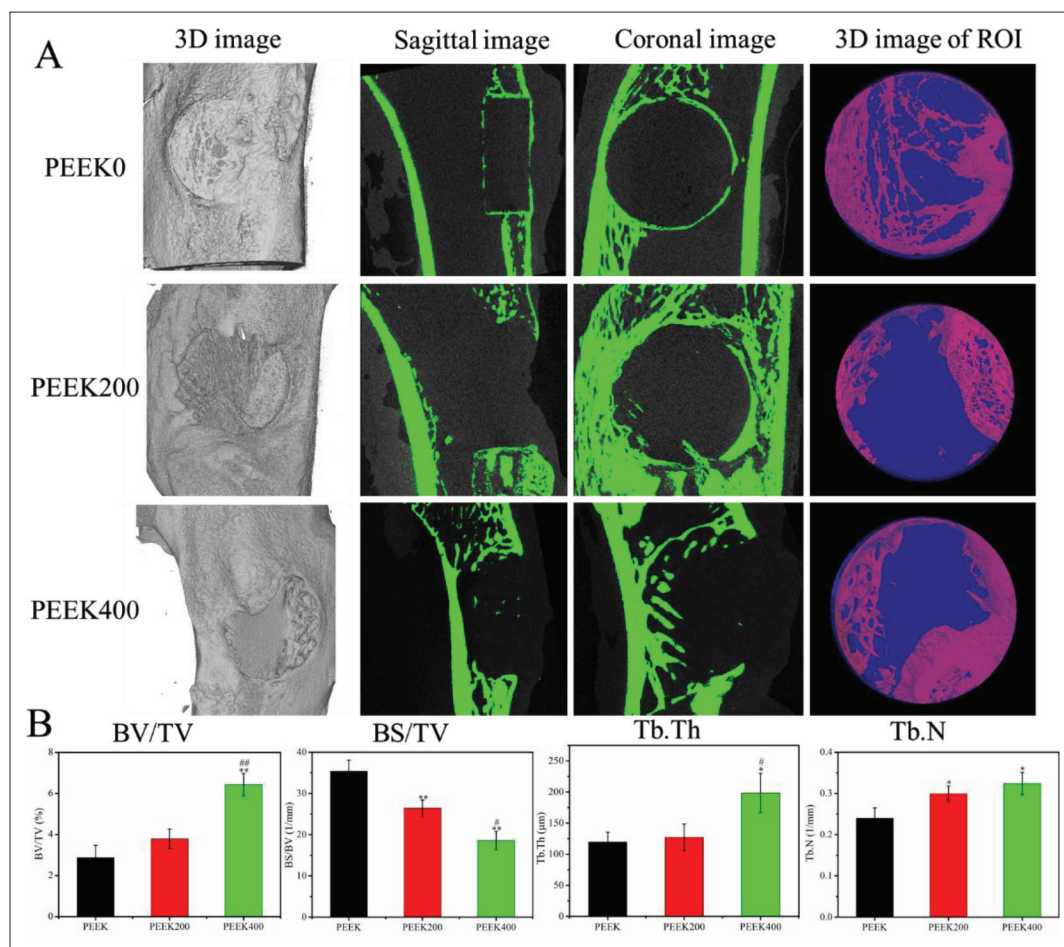


**Figure 7.** Micro-CT evaluation of the repaired tibial defect after 12 weeks of implantation. (A) 3D image, sagittal image, coronal image, and 3D image of region of interest (ROI) of micro-CT. (B) Quantitative analysis of bone volume/total volume ratio (BV/TV), bone surface/bone volume (BS/BV), trabecular thickness (Tb. Th), and trabecular number (Tb. N) from micro-CT data. Data are shown as the mean  $\pm$  SD for  $n \geq 3$ ; \* $p < 0.05$ , \*\* $p < 0.01$ , and \*\*\* $p < 0.001$  indicate significant differences when compared to the PEEK0; # $p < 0.05$ , ## $p < 0.01$ , and ### $p < 0.001$  indicate significant differences when compared to the PEEK200.

formation has been fully demonstrated<sup>[35-37]</sup>. However, since macrophage polarization is affected by material properties (including pore size) and polarized macrophages can play corresponding functions, pore size is likely to mediate macrophage polarization and affect subsequent angiogenesis and new bone formation<sup>[17,19]</sup>. To test this hypothesis, 3D-printed PEEK scaffolds with different pore sizes (0, 200, and 400  $\mu\text{m}$ ) were designed, and their effects on macrophage polarization and subsequent angiogenesis and osteogenesis were tested *in vitro* and *in vivo*.

PEEK is a promising bone replacement material because of its good chemical resistance, thermal stability, elastic modulus, and mechanical behavior similar to human cortical bone<sup>[38,39]</sup>. In addition, 3D printing technology is suitable for the fabrication of personalized PEEK bone repair materials, and the control of the pore size and porosity of the scaffold can be achieved by optimizing different parameters. In this study, PEEK

scaffolds with different pore sizes were prepared by fused deposition modeling (FDM) 3D printing technology, and the differences between the scaffolds were only reflected in the pore size and porosity, but had the same chemical and physical properties. Therefore, 3D-printed PEEK scaffolds with different pore sizes were used as models to study the effect of the pore size of the scaffolds on macrophages.

To test if macrophages respond to the pore size of the scaffold, PCR and ELISA were used to detect macrophage polarization-related genes and cytokines after co-culture of macrophages with scaffolds. Gene expression results showed that, compared with the PEEK group, the expression levels of M1 macrophage-related genes (*iNOS* and *NF- $\kappa$ B*) in the PEEK400 group were relatively low, and the expression levels of M2 macrophage-related genes (*CD206*, *TGF- $\beta$* , and *IL-10*) were significantly higher, which demonstrated that macrophages co-cultured with scaffolds with larger pore sizes were more inclined to polarize toward M2-

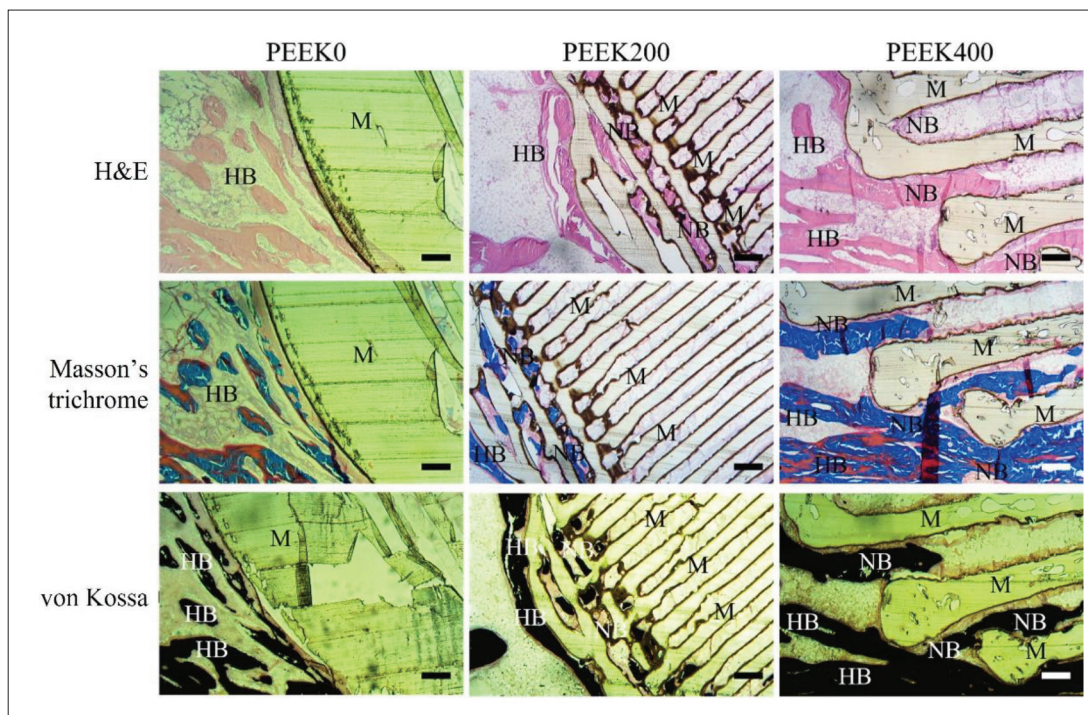


**Figure 8.** New bone formation after 12 weeks of implantation of scaffolds with different pore sizes into rabbit tibial defects. Representative images of histological slices stained with H&E, Masson's trichrome, and von Kossa staining (scale bar = 200  $\mu$ m). Abbreviations: HB, host bone; NB, new bone; RM, residual material.

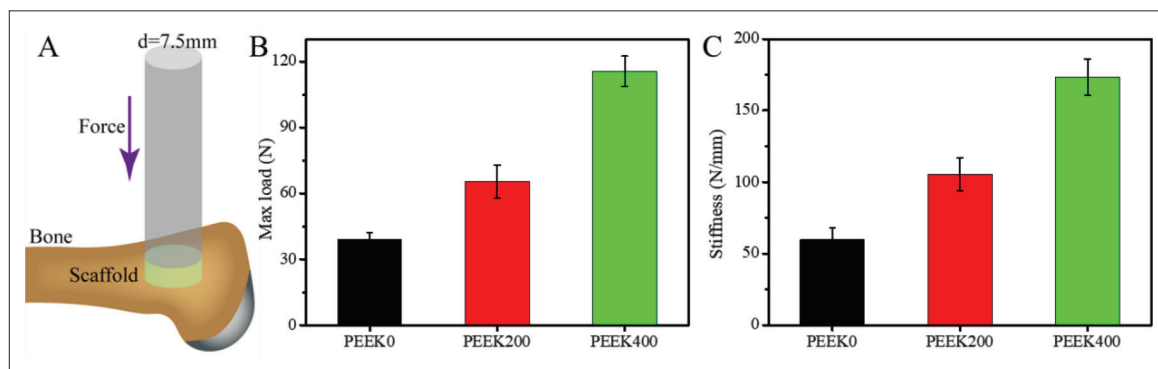


**Figure 9.** Biomechanical test of the repaired tibial defect after 12 weeks of implantation. Schematic diagram of biomechanical test (A), maximum load (B), and stiffness of tibial specimens (C). Data are shown as the mean  $\pm$  SD for  $n \geq 3$ ; \* $p < 0.05$ , \*\* $p < 0.01$ , and \*\*\* $p < 0.001$  indicate significant differences when compared to the PEEK0; \* $p < 0.05$ , \*\* $p < 0.01$ , and \*\*\* $p < 0.001$  indicate significant differences when compared to the PEEK200.

type macrophages. In the process of recognizing material properties and polarizing into different phenotypes, macrophages release a large number of cytokines, which can then perform different functions<sup>[15,40]</sup>. ELISA results showed that macrophages seeded on PEEK400 scaffolds secreted more M2-related cytokines (TGF $\beta$ , IL-10, or insulin-like growth factor [IGF]) and less M1-related cytokines (IL-6) than macrophages seeded on PEEK0 scaffold. In addition, PEEK400 scaffolds with larger pore size had the highest concentrations of osteogenesis-related factor BMP-2 and angiogenesis-related factor PDGF-

bb<sup>[14,27,41]</sup>. The pore size of the scaffold has no effect on the degree of inflammatory response of macrophages, but the scaffold with larger pore size can promote the anti-inflammatory effect of macrophages and increase the release of osteogenesis- and angiogenesis-related factors.

The effects of CM obtained by co-culture of macrophages with scaffolds on scratch healing and angiogenesis-related gene expression in HUVECs were evaluated *in vitro*. The wound healing results showed that the CM in the PEEK400 group was more able to promote

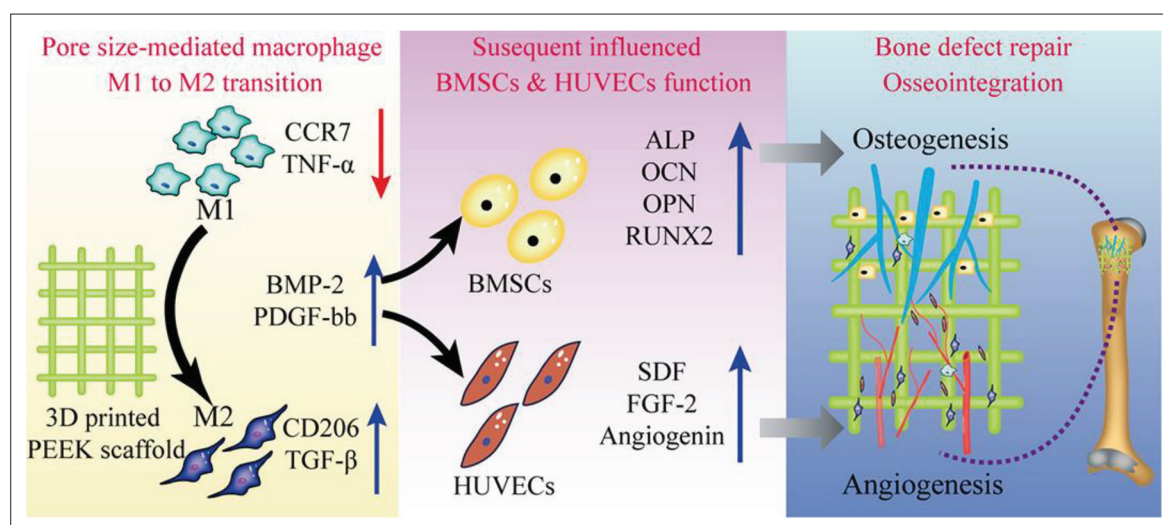


**Figure 10.** Schematic diagram of 3D-printed PEEK scaffolds with different pore sizes regulating macrophage polarization to promote osseointegration. Macrophages can respond to the changes of scaffold pore size, and the increase in scaffold pore size can promote macrophage M1 to M2 phenotype transition, while promoting angiogenesis of HUVECs and osteogenic differentiation of BMSCs *in vitro*, and subsequently enhancing scaffold osseointegration.

the migration of HUVECs, thereby promoting the healing of scratches. The angiogenesis-related gene expression results of HUVECs cultured in CM for 3 days showed that the expressions of *Angiogenin* and *SDF* genes in PEEK400 group were significantly higher than those in PEEK0 and PEEK200 groups. The results indicated that the CM of the scaffold group with larger pore size had a significant *in vitro* pro-angiogenic effect, which was closely related to the vascular-associated PDGF-bb growth factor released by macrophages<sup>[12,34,42]</sup>.

The results of ALP staining and its quantification indicated that BMSCs cultured in the CM of PEEK400 scaffolds had the strongest ALP activity, and the trend of Alizarin red S staining and osteogenesis-related gene expression results were consistent with the ALP results. Because PEEK400 scaffold group can promote macrophage polarization and secrete high concentrations of osteogenesis-related cytokines (BMP-2, PDGF-bb, etc.), we believe that the immune microenvironment induced by macrophages co-cultured with PEEK with larger pore size is beneficial to the osteogenic differentiation of BMSCs<sup>[43-45]</sup>. Further, the osseointegration effect of PEEK scaffolds with different pore sizes was investigated using a rabbit tibial defect model. Micro-CT 2D images and 3D reconstruction showed that compared with the PEEK0 group, the PEEK400 group had significantly more new bone around and inside the material, and its bone mineral density, BV/TV, and Tb.N values also increased significantly. Furthermore, with the increase of the pore size of the scaffold, there is a greater amount of new and more mature bone inside the scaffold (Figure 8). In addition, the biomechanical results showed that the maximum load

and stiffness of the PEEK400 scaffold were higher, which further indicated that the PEEK scaffold with larger pore size had better osseointegration performance with the host bone.

Macrophages are sensitive to the pore size of the scaffold, and PEEK scaffolds with larger pore size can induce the polarization of macrophages from M1 type to M2 type, and promote the angiogenesis of HUVECs and the osteogenic differentiation of BMSCs *in vitro* (Figure 10). Furthermore, the PEEK scaffold with larger pore size promotes the formation and growth of new bone, thereby achieving a better osseointegration effect. Therefore, the results of this study demonstrated that the strategy of mediating macrophages to promote osseointegration of PEEK scaffolds by regulating the pore size of the scaffolds is feasible, but future research based on bionic design of natural bone tissue and precise control of material structure is warranted. In addition, the reason for the M1 to M2 transition mediated by the aperture of 3D printing PEEK scaffold is still unclear. In future research, we also need to explore how the pore size of the scaffold, or the micro-nano multi-level structure of the scaffold, affects other immune cells in the immune system, and then affects the integration of PEEK scaffold and host bone.

## 5. Conclusion

PEEK scaffolds with pore sizes of 0, 200, and 400  $\mu\text{m}$  were prepared by FDM 3D printing technology, and the pore size-mediated macrophage polarization and its effects on subsequent angiogenesis, bone regeneration, and osseointegration were studied. Our data suggest that

compared to scaffolds with small pore size, scaffolds with large pore size induce a higher degree of M1 to M2 transition of macrophages and promote angiogenesis of HUVECs and osteogenic differentiation of BMSCs *in vitro*. In addition, scaffolds with large pore size promote the formation and ingrowth of new bone *in vivo*, thereby achieving a better osseointegration effect. This study explores the potential relationship between pore size, macrophage function, and osseointegration of PEEK scaffolds, which may provide a new strategy for promoting osseointegration of PEEK bone repair materials with host bone.

## Acknowledgments

None.

## Funding

This work was supported by National Natural Science Foundation of China (Grant No. 82002286), Guangdong Science and Technology Planning Project (Grant No. 2020A1515111041), and Henan Medical Science and Technology Provincial and Ministry co-construction research project (Grant No. SBGJ202102089).

## Conflict of interest

The authors declare no conflict of interest.

## Author contributions

*Conceptualization:* Xiaopeng Yang, Dichen Li

*Data curation:* Xiaopeng Yang, Shenyu Yang, Huilong Liu, Danyang Su

*Formal analysis:* Xiaopeng Yang, Shenyu Yang

*Funding acquisitions:* Xiaopeng Yang, Shenyu Yang, Dichen Li

*Investigation:* Xiaopeng Yang, Huilong Liu, Danyang Su

*Methodology:* Xiaopeng Yang

*Project administration:* Dichen Li

*Resources:* Xiaopeng Yang, Dichen Li, Jianbo Gao, Yan Wu

*Supervision:* Dichen Li, Jianbo Gao

*Visualization:* Xiaopeng Yang, Shenyu Yang

*Writing – original draft:* Xiaopeng Yang, Shenyu Yang

*Writing – review & editing:* Xiaopeng Yang, Shenyu Yang, Dichen Li

## Ethics approval and consent to participate

Ethical approval was obtained from the Experimental Animal Ethics Committee of Jinan University (20210426-02).

## Consent for publication

Not applicable.

## Availability of data

The data that support the findings of this study can be acquired from the corresponding author upon reasonable request.

## Reference

1. Alves A, Thibeaux R, Toptan F, *et al.*, 2019, Influence of macroporosity on NIH/3T3 adhesion, proliferation, and osteogenic differentiation of MC3T3-E1 over bio-functionalized highly porous titanium implant material. *J Biomed Mater Res Part B*, 107(1): 73–85.
2. Chen Z, Bachhuka A, Wei F, *et al.*, 2017, Nanotopography-based strategy for the precise manipulation of osteoimmunomodulation in bone regeneration. *Nanoscale*, 9(46): 18129–18152.
3. Trindade R, Albrektsson T, Tengvall P, *et al.*, 2016, Foreign body reaction to biomaterials: On mechanisms for buildup and breakdown of osseointegration. *Clin Implant Den Relat Res*, 18(1): 192–203.
4. Zhang D, Chen Q, Shi C, *et al.*, 2021, Dealing with the foreign-body response to implanted biomaterials: strategies and applications of new materials. *Adv Funct Mater*, 31(6): 2007226.
5. Balabiyev A, Podolnikova NP, Kilbourne JA, *et al.*, 2021, Fibrin polymer on the surface of biomaterial implants drives the foreign body reaction. *Biomaterials*, 277: 121087.
6. Niu Y, Wang Z, Shi Y, *et al.*, 2021, Modulating macrophage activities to promote endogenous bone regeneration: Biological mechanisms and engineering approaches. *Bioact Mater*, 6(1): 244–261.
7. Schlundt C, Fischer H, Bucher CH, *et al.*, 2021, The multifaceted roles of macrophages in bone regeneration: A story of polarization, activation and time. *Acta Biomater*, 133: 46–57.
8. Xie Y, Hu C, Feng Y, *et al.*, 2020, Osteoimmunomodulatory effects of biomaterial modification strategies on macrophage polarization and bone regeneration. *Regen Biomater*, 7(3): 233–245.
9. Kim H, Wang SY, Kwak G, *et al.*, 2019, Exosome-guided phenotypic switch of M1 to M2 macrophages for cutaneous wound healing. *Adv Sci*, 6(20): 1900513.
10. Graney P, Ben-Shaul S, Landau S, *et al.*, 2020, Macrophages of diverse phenotypes drive vascularization of engineered tissues. *Sci Adv*, 6(18): eaay6391.
11. Zhang W, Zhao F, Huang D, 2016, Strontium-substituted submicrometer bioactive glasses modulate macrophage responses for improved bone regeneration. *ACS Appl Mater Interfaces*, 8(45): 30747–30758.
12. Spiller KL, Anfang RR, Spiller KJ, *et al.*, 2014, The role of macrophage phenotype in vascularization of tissue engineering scaffolds. *Biomaterials*, 35(15): 4477–4488.

13. Sun J-l, Jiao K, Niu L-n, *et al.*, 2017, Intrafibrillar silicified collagen scaffold modulates monocyte to promote cell homing, angiogenesis and bone regeneration. *Biomaterials*, 113: 203–216.
14. Spiller KL, Nassiri S, Witherel CE, *et al.*, 2015, Sequential delivery of immunomodulatory cytokines to facilitate the M1-to-M2 transition of macrophages and enhance vascularization of bone scaffolds. *Biomaterials*, 37: 194–207.
15. Yang C, Ouyang L, Wang W, *et al.*, 2019, Sodium butyrate-modified sulfonated polyetheretherketone modulates macrophage behavior and shows enhanced antibacterial and osteogenic functions during implant-associated infections. *J Mater Chem B*, 7(36): 5541–5553.
16. Han J, Kim YS, Lim M-Y, *et al.*, 2018, Dual roles of graphene oxide to attenuate inflammation and elicit timely polarization of macrophage phenotypes for cardiac repair. *ACS Nano*, 12(2): 1959–1977.
17. Garg K, Pullen NA, Oskeritzian CA, *et al.*, 2013, Macrophage functional polarization (M1/M2) in response to varying fiber and pore dimensions of electrospun scaffolds. *Biomaterials*, 34(18): 4439–4451.
18. Luu TU, Gott SC, Woo BW, *et al.*, 2015, Micro-and nanopatterned topographical cues for regulating macrophage cell shape and phenotype. *ACS Appl Mater Interfaces*, 7(51): 28665–28672.
19. Sussman EM, Halpin MC, Muster J, *et al.*, 2014, Porous implants modulate healing and induce shifts in local macrophage polarization in the foreign body reaction. *Ann Biomed Eng*, 42(7): 1508–1516.
20. Dong T, Duan C, Wang S, *et al.*, 2020, Multifunctional surface with enhanced angiogenesis for improving long-term osteogenic fixation of poly (ether ether ketone) implants. *ACS Appl Mater Interfaces*, 12(13): 14971–14982.
21. Liu X, Ouyang L, Chen L, *et al.*, 2022, Hydroxyapatite composited PEEK with 3D porous surface enhances osteoblast differentiation through mediating NO by macrophage. *Regen Biomater*, 9.
22. Kim J, Cao Y, Eddy C, *et al.*, 2021, The mechanics and dynamics of cancer cells sensing noisy 3D contact guidance. *Proc Natl Acad Sci*, 118(10): e2024780118.
23. Gao C, Wang Z, Jiao Z, *et al.*, 2021, Enhancing antibacterial capability and osseointegration of polyetheretherketone (PEEK) implants by dual-functional surface modification. *Mater Des*, 205: 109733.
24. Xue Z, Wang Z, Huang J, *et al.*, 2020, Rapid construction of polyetheretherketone (PEEK) biological implants incorporated with brushite (CaHPO<sub>4</sub>·2H<sub>2</sub>O) and antibiotics for anti-infection and enhanced osseointegration. *Mater Sci Eng C*, 111: 110782.
25. Torstrick FB, Lin AS, Potter D, *et al.*, 2018, Porous PEEK improves the bone-implant interface compared to plasma-sprayed titanium coating on PEEK. *Biomaterials*, 185: 106–116.
26. Ding R, Chen T, Xu Q, *et al.*, 2019, Mixed modification of the surface microstructure and chemical state of polyetheretherketone to improve its antimicrobial activity, hydrophilicity, cell adhesion, and bone integration. *ACS Biomater Sci Eng*, 6(2): 842–851.
27. Yin Y, He X-T, Wang J, *et al.*, 2020, Pore size-mediated macrophage M1-to-M2 transition influences new vessel formation within the compartment of a scaffold. *Appl Mater Today*, 18: 100466.
28. Wu R, Li Y, Shen M, *et al.*, 2021, Bone tissue regeneration: The role of finely tuned pore architecture of bioactive scaffolds before clinical translation. *Bioact Mater*, 6(5): 1242–1254.
29. Liang C-C, Park AY, Guan J-L, 2007, In vitro scratch assay: A convenient and inexpensive method for analysis of cell migration in vitro. *Nat Protoc*, 2(2): 329–333.
30. Loi F, Córdova LA, Pajarinen J, 2016, Inflammation, fracture and bone repair. *Bone*, 86: 119–130.
31. Qiu P, Li M, Chen K, *et al.*, 2020, Periosteal matrix-derived hydrogel promotes bone repair through an early immune regulation coupled with enhanced angio-and osteogenesis. *Biomaterials*, 227: 119552.
32. Yang C, Zhao C, Wang X, *et al.*, 2019, Stimulation of osteogenesis and angiogenesis by micro/nano hierarchical hydroxyapatite via macrophage immunomodulation. *Nanoscale*, 11(38): 17699–17708.
33. Aplin AC, Ligresti G, Fogel E, 2014, Regulation of angiogenesis, mural cell recruitment and adventitial macrophage behavior by Toll-like receptors. *Angiogenesis*, 17(1): 147–161.
34. Zhao F, Lei B, Li X, *et al.*, 2018, Promoting in vivo early angiogenesis with sub-micrometer strontium-contained bioactive microspheres through modulating macrophage phenotypes. *Biomaterials*, 178: 36–47.
35. Bobbert F, Zadpoor A. Effects of bone substitute architecture and surface properties on cell response, angiogenesis, and structure of new bone. *J Mater Chem B*, 5(31): 6175–6192.
36. Li J, Zhi W, Xu T, *et al.*, 2016, Ectopic osteogenesis and angiogenesis regulated by porous architecture of hydroxyapatite scaffolds with similar interconnecting structure in vivo. *Regen Biomater*, 3(5): 285–297.
37. Diao J, Ding H, Huang M, *et al.*, 2019, Bone defect model dependent optimal pore sizes of 3D-plotted beta-tricalcium phosphate scaffolds for bone regeneration. *Small Methods*, 3(11): 1900237.
38. Ji Y, Zhang H, Ru J, *et al.*, 2021, Creating micro-submicro structure and grafting hydroxyl group on PEEK by femtosecond laser and hydroxylation to synergistically activate cellular response. *Mater Des*, 199: 109413.
39. Dey S, Sen I, Samanta S, 2021, Mechanical characterisation of PEEK-HA composite as an orthopaedic implant. *Adv Mater Process Technol*, 1–24.



40. Mahon OR, Browe DC, Gonzalez-Fernandez T, *et al.*, 2020, Nano-particle mediated M2 macrophage polarization enhances bone formation and MSC osteogenesis in an IL-10 dependent manner. *Biomaterials*, 239: 119833.
41. Das S, Majid M, Baker AB, 2016, Syndecan-4 enhances PDGF-BB activity in diabetic wound healing. *Acta Biomater*, 42: 56–65.
42. Guo S, Yu D, Xiao X, *et al.*, 2020, A vessel subtype beneficial for osteogenesis enhanced by strontium-doped sodium titanate nanorods by modulating macrophage polarization. *J Mater Chem B*, 8(28): 6048–6058.
43. Wang M, Yu Y, Dai K, *et al.*, 2016, Improved osteogenesis and angiogenesis of magnesium-doped calcium phosphate cement via macrophage immunomodulation. *Biomater Sci*, 4(11): 1574–1583.
44. Zhang Y, Böse T, Unger RE, *et al.*, 2017, Macrophage type modulates osteogenic differentiation of adipose tissue MSCs. *Cell Tissue Res*, 369(2): 273–286.
45. Chen Z, Wu C, Gu W, *et al.*, 2014, Osteogenic differentiation of bone marrow MSCs by  $\beta$ -tricalcium phosphate stimulating macrophages via BMP2 signalling pathway. *Biomaterials*, 35(5): 1507–1518. Author Queries